Supplementary Data

Supplementary Figure 1

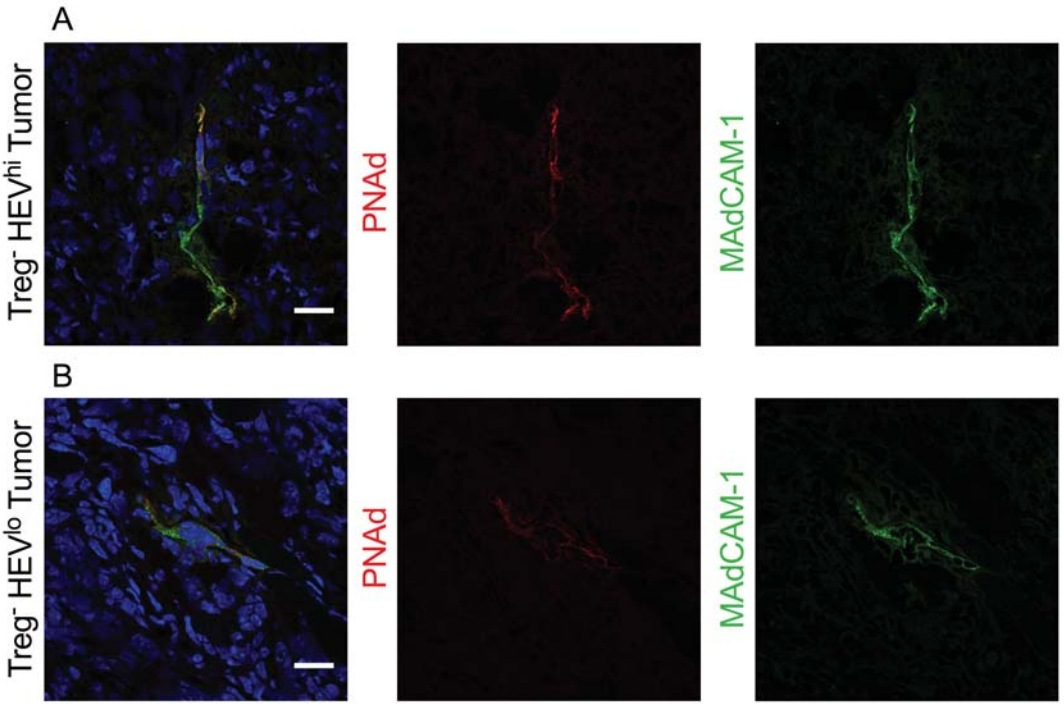

Supplementary Figure 1. Tumor HEV identified by PNAd staining are also positive for MAdCAM-1
(A) Representative high power images of HEV (PNAd; red, MAdCAM1; green, nuclear stain DAPI; blue) in frozen tumors from Treg^{-}HEV^{hi} (A) and Treg^{-} HEV^{lo} (B) tumors. Scale bars represent 20μm.

Supplementary Figure 2

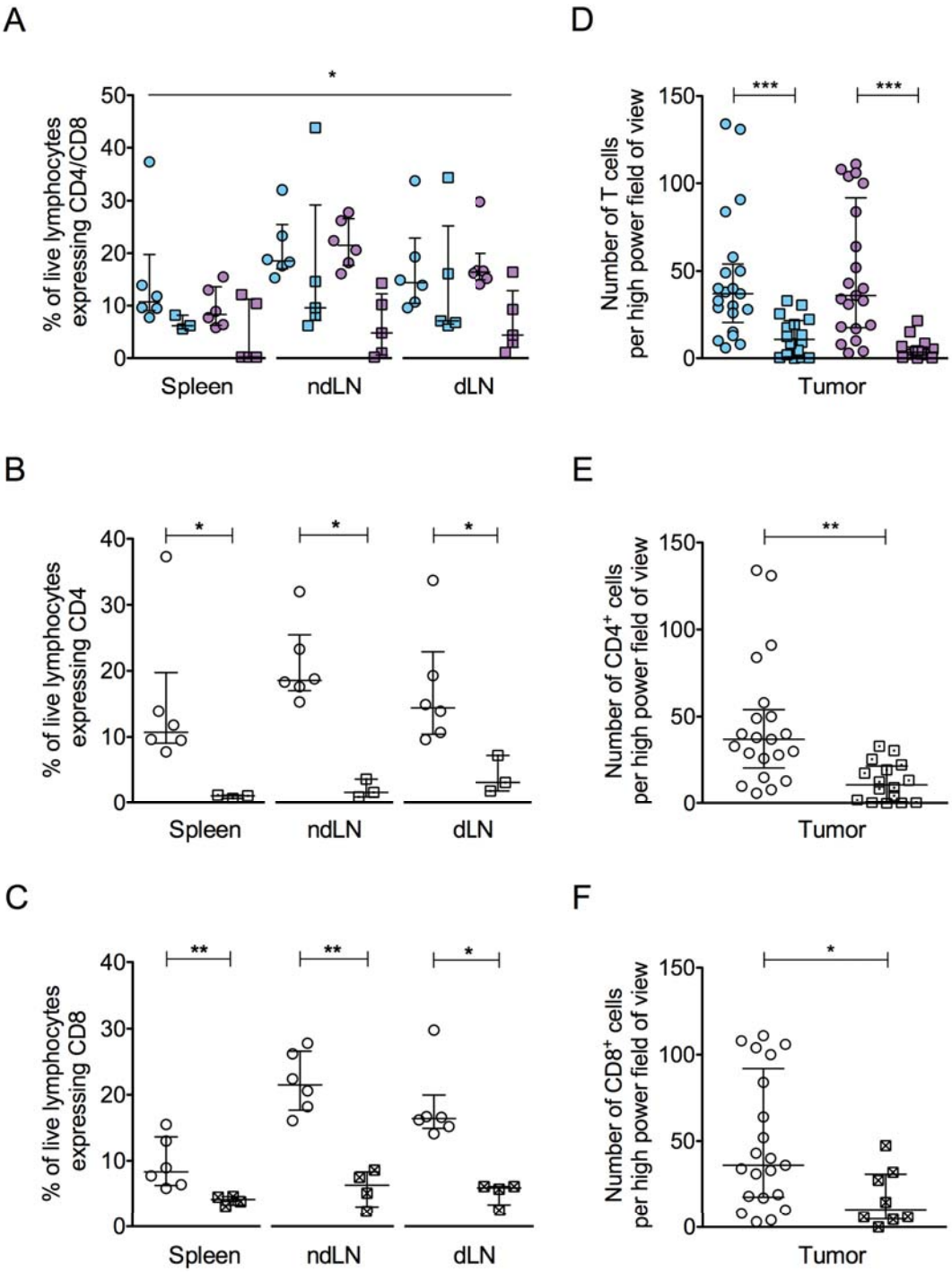

Supplementary Figure 2. Efficacy of monoclonal antibody treatments to deplete immune cell subsets
(A-C) Proportion of live lymphocytes expressing CD4 or CD8 in spleen, non tumor-draining lymph node (ndLN), and tumor-draining lymph node (dLN), determined by flow cytometry in Treg-depleted and anti-CD4/CD8 treated ($Treg^-$ + anti-CD4/CD8; A; N = 3), Treg-depleted and anti-CD4 treated ($Treg^-$ + anti-CD4; B; N = 3), or Treg-depleted and anti-CD8 treated ($Treg^-$ + anti-CD8; C; N = 4), relative to Treg-depleted ($Treg^-$; circles) $Foxp3^{DTR}$ animals at the end of treatment.
(D-F) Counts of immune cells per high power field of view for tumors of Treg-depleted and anti-CD4/CD8 treated ($Treg^-$ + anti-CD4/CD8; D; N = 16), Treg-depleted and anti-CD4 treated ($Treg^-$ + anti-CD4; E; N = 11), or Treg-depleted and anti-CD8 treated ($Treg^-$ + anti-CD8; F; N = 8), relative to Treg-depleted ($Treg^-$; circles; N = 12) $Foxp3^{DTR}$ animals at the end of treatment. Data are presented as median ± Interquartile range. Statistical significance was determined by Mann Whitney *t* tests.

Supplementary Figure 3

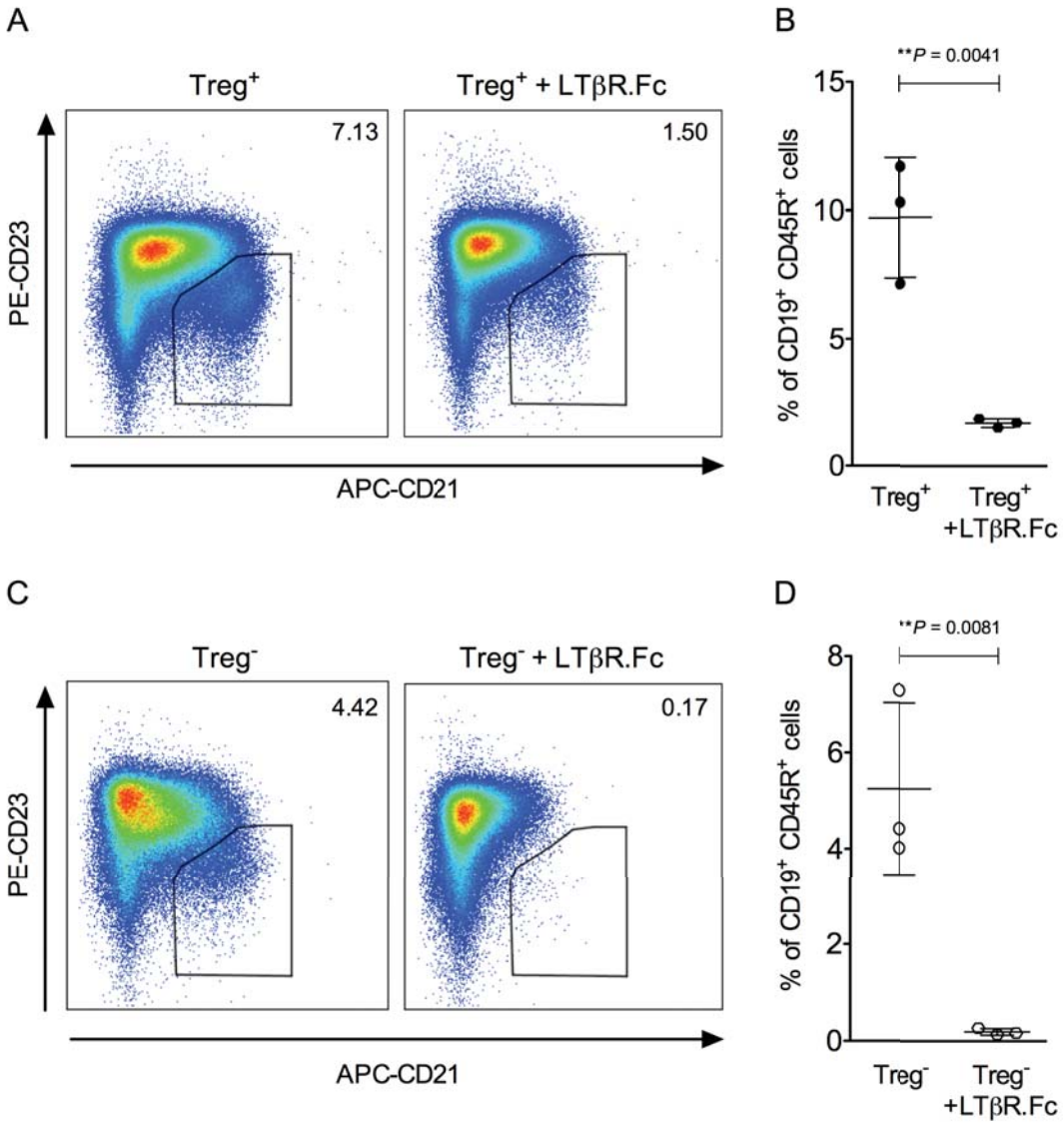

Supplementary Figure 3. Splenic Marginal Zone B cells are profoundly decreased after treatment with LTβR.Fc

(A-B) Representative flow cytometry plots showing the proportion of $CD19^+$ $CD45R^+$ B cells that are $CD21^{hi}$ $CD23^{lo}$ Marginal Zone (MZ) B cells, in the spleen of Treg-replete ($Treg^+$) and Treg-replete LTβR.Fc treated ($Treg^+$ + LTβR.Fc) $Foxp3^{DTR}$ animals (left, right, respectively; A), or Treg-depleted ($Treg^-$) and Treg-depleted LTβR.Fc treated ($Treg^-$ + LTβR.Fc) $Foxp3^{DTR}$ animals (left, right, respectively; B). Cells are gated on $CD19^+$, $CD45R^+$. Numbers represent MZ B cells (gated), as a proportion of live $CD19^+$ $CD45R^+$ B cells. Expression of CD23 is shown on the y-axis; expression of CD21 is shown on the x-axis. (C-D) Proportion of $CD19^+$ $CD45R^+$ B cells that are $CD21^{hi}$ $CD23^{lo}$ MZ B cells (left hand graphs) in spleen of Treg-replete ($Treg^+$) and Treg-replete LTβR.Fc treated ($Treg^+$ + LTβR.Fc) $Foxp3^{DTR}$ animals (C) or Treg-depleted ($Treg^-$) and Treg-depleted LTβR.Fc treated ($Treg^-$ + LTβR.Fc) $Foxp3^{DTR}$ animals (D). Data are presented as individual data points and mean ± Standard Deviation (SD). Statistical significance was determined by unpaired *t* tests. N = 3 per group.

Supplementary Figure 4

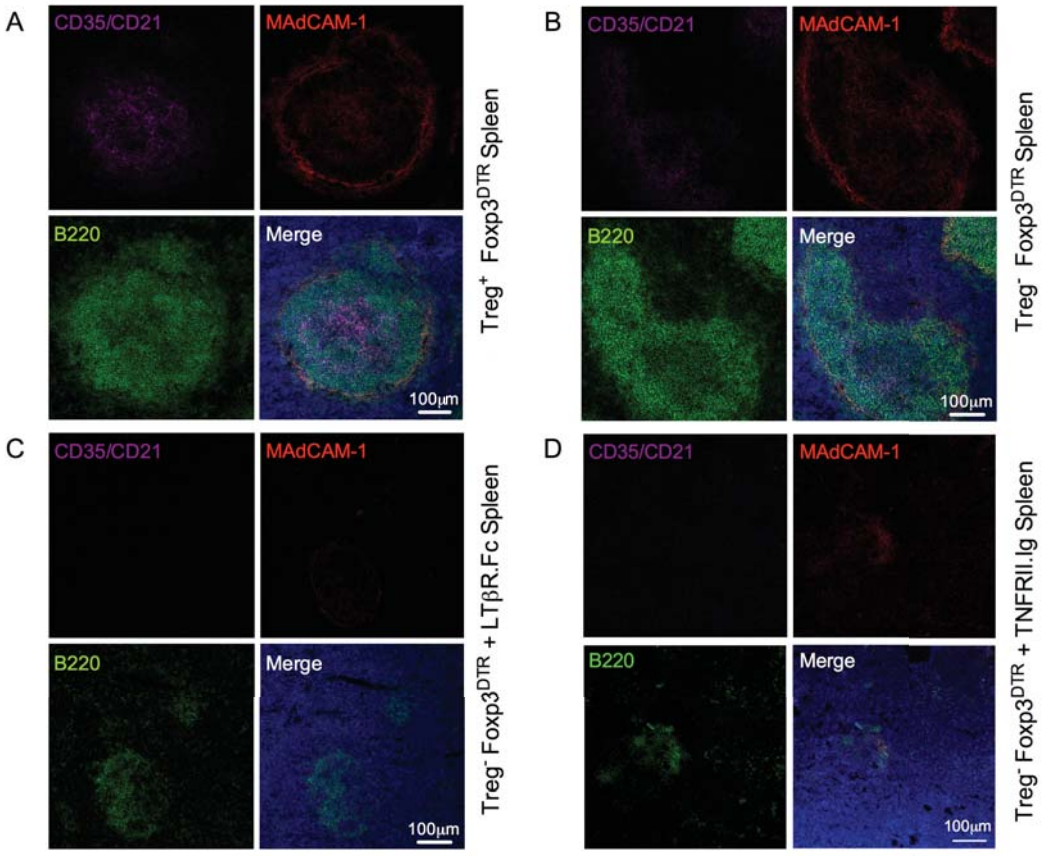

Supplementary Figure 4. Splenic Follicular Dendritic Cells and MAdCAM-1 staining are lost after treatment with LTβR.Fc or TNFRII.Ig

Representative high power images of Follicular Dendritic Cells (FDCs; CD35/CD21; purple), and MAdCAM-1 staining of marginal sinus-lining stromal cells (red) around B cells follicles (B220; green) in the Spleen of Treg-replete ($Treg^+$; A), Treg-depleted ($Treg^-$; B), Treg-depleted, LTβR.Fc treated ($Treg^-$ + LTβR.Fc; C), and Treg-depleted, TNFRII.Ig treated ($Treg^-$ + TNFRII.Ig; D) $Foxp3^{DTR}$ animals. Merged images include the nuclear stain DAPI (blue).

Supplementary Figure 5

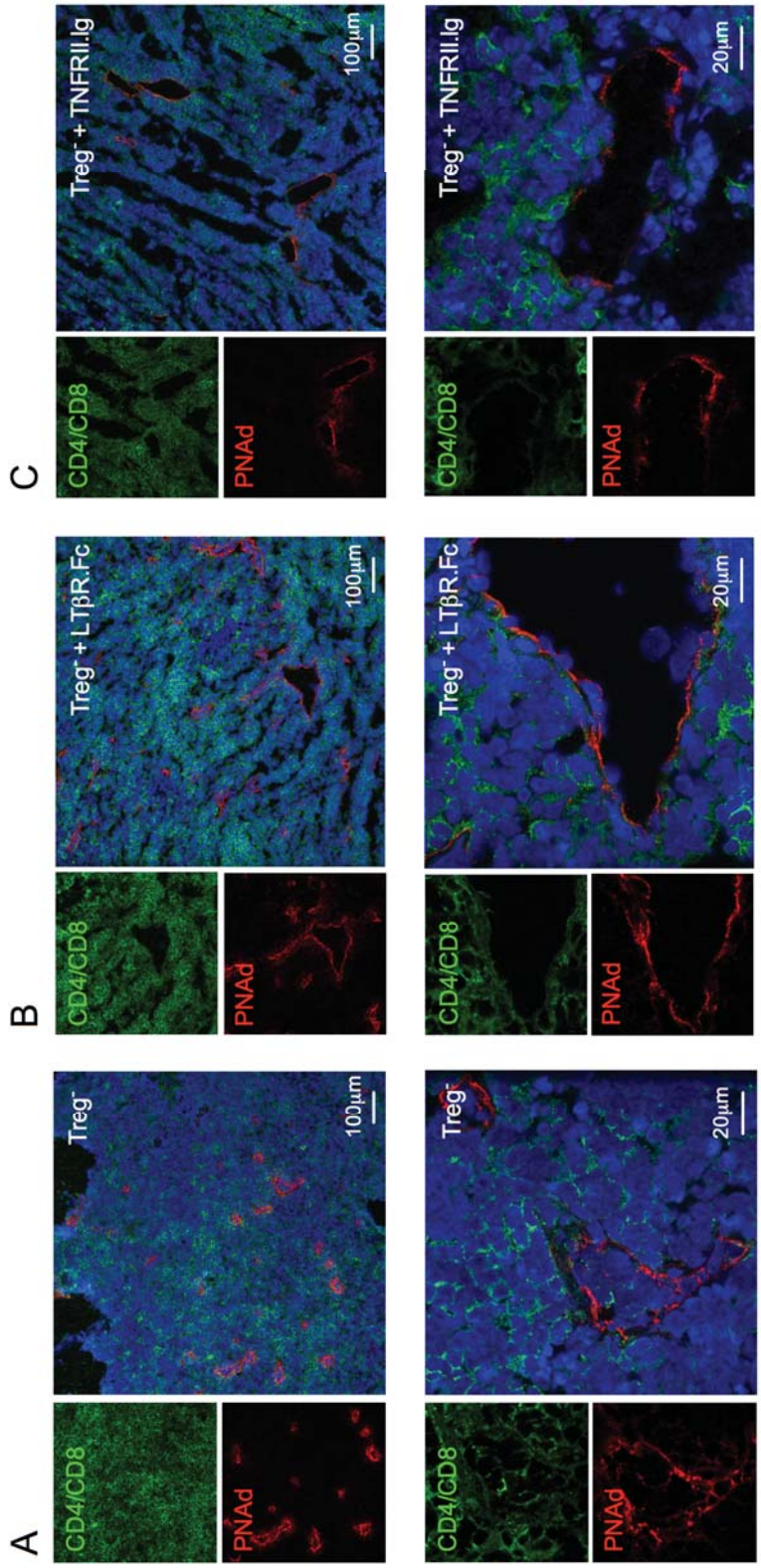

Supplementary Figure 5. Lymph Node architecture is disrupted following treatment with LTβR.Fc or TNFRII.Ig

Representative low power (top panels) and high power (lower panels) images of HEV (PNAd; red) and T cells (CD4/CD8; green) in Lymph Nodes of Treg-depleted ($Treg^-$; A), Treg-depleted, LTβR.Fc treated ($Treg^-$ + LTβR.Fc; B), and Treg-depleted, TNFRII.Ig treated ($Treg^-$ + TNFRII.Ig; C) $Foxp3^{DTR}$ animals. Merged images include the nuclear stain DAPI (blue).

Supplementary Figure 6

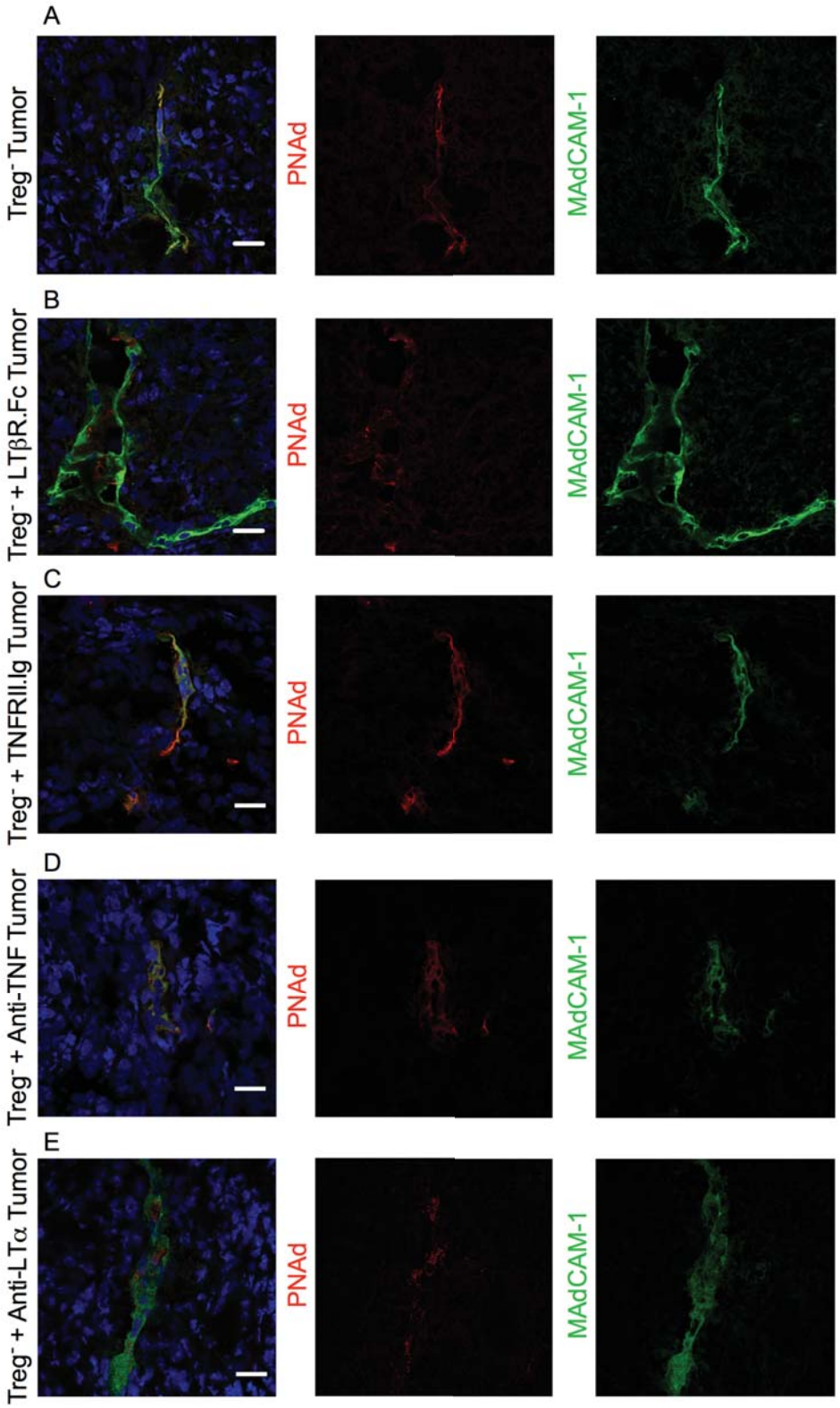

Supplementary Figure 6. Tumor HEV identified by PNAd staining following blockade of LTβR or TNFR signalling are also positive for MAdCAM-1

Representative high power images of HEV (PNAd; red, MAdCAM1; green, nuclear stain DAPI; blue) in frozen tumors from Treg⁻ (A; as shown in Supplementary Figure 1) Treg⁻ + LTβR.Fc (B), Treg⁻ + TNFRII.Ig (C), Treg⁻ + anti-TNF (D), and Treg⁻ + anti-LTα (E) tumors. Scale bars represent 20μm.

Supplementary Figure 7

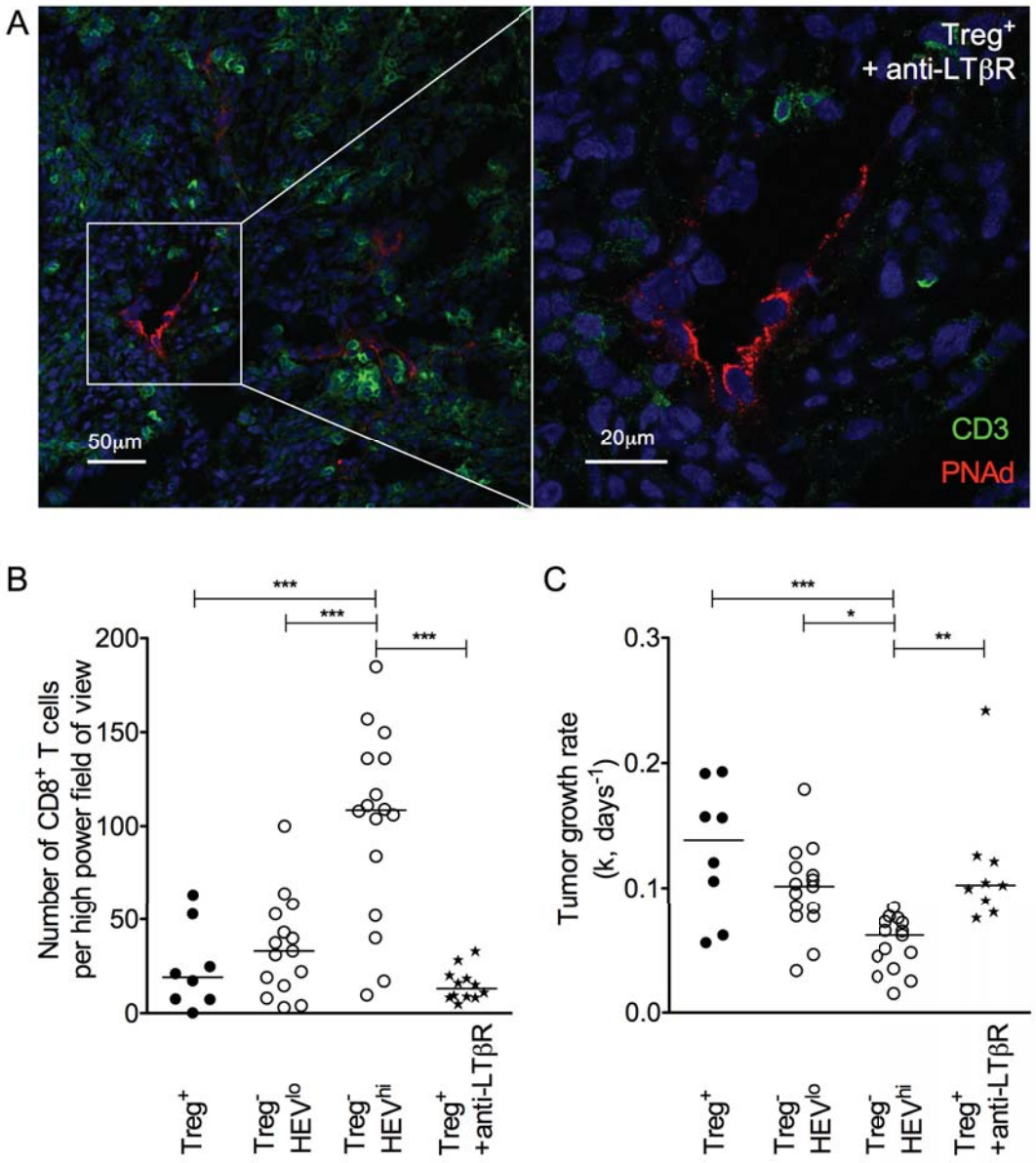

Supplementary Figure 7. Agonism of LTβR induces formation of High Endothelial Venules in Treg replete tumors, but without concomitant increased T cell infiltration and reduced tumor growth
(A) Representative low and high power images of HEV (PNAd; red) alongside T cells (CD3; green) in a tumor of a Treg replete Foxp3^{DTR} animal treated with agonistic anti-LTβR antibody (Treg^{+} + anti-LTβR). Merged images include the nuclear stain DAPI (blue). (B) Number of CD8^{+} T cells in tumors of Treg^{+} (N = 8), Treg^{-} HEV^{-} (N = 12), Treg^{-} HEV^{+} (N = 14), and Treg^{+} anti-LTβR treated Foxp3^{DTR} animals (N = 12). (C) Tumor growth rates (k, days^{-1}) for Treg^{+} (N = 8), Treg^{-} HEV^{-} (N = 12), Treg^{-} HEV^{+} (N = 13), and Treg^{+} anti-LTβR treated Foxp3^{DTR} animals (N = 9). Statistical significance was determined by One-Way ANOVA with Tukey's tests to compare pairs of means (* = $P \leq 0.05$, ** = $P \leq 0.01$, *** = $P \leq 0.001$).

Supplementary Figure 8

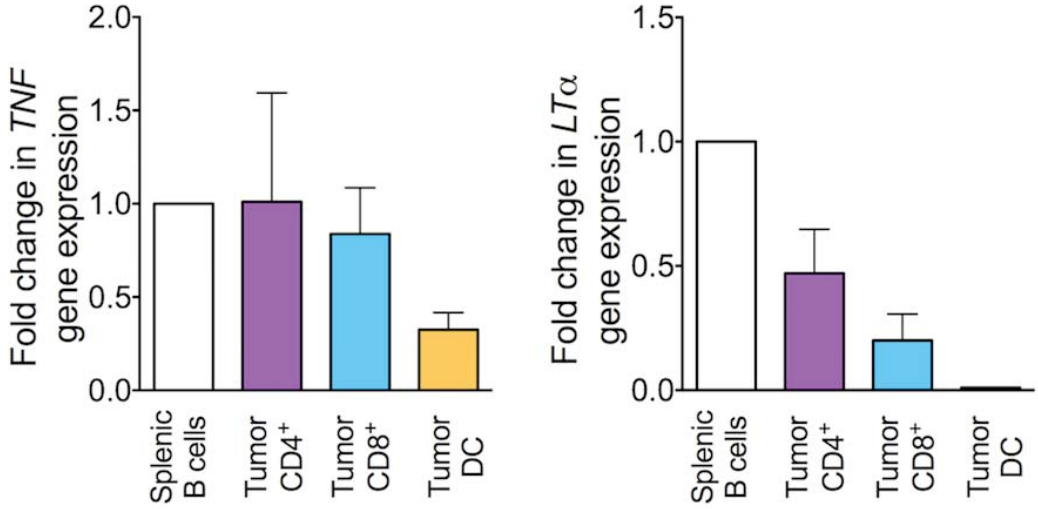

Supplementary Figure 8. Relative gene expression of *TNF* and *LTα* by intratumoral $CD4^+$ and $CD8^+$ T cells and dendritic cells (DC). Data are expressed as fold change in gene expression relative to splenic B cells, and represent two independent experiments.